DAΦNE TECHNICAL NOTE

INFN - LNF, Accelerator Division

Frascati, Feb. 11, 1991

Note: **LC-1**

THE LINEAR ACCELERATOR FOR THE DAΦNE INJECTION SYSTEM

S. Kulinski, R. Boni, B. Spataro, M. Vescovi, G. Vignola

1 - INTRODUCTION

The purpose of this note is to define the specifications of the LINAC for the DAΦNE Injection System (IS).

The normal operation for DAΦNE contemplates a single full injection followed by topping-up, in order to increase the integrated luminosity. It is prudent to dimension the IS performances for the maximum current (≈ 5 Amp) that one can reasonably assume to store into the storage rings [1]. If we put an upper limit ~ 5 minutes on the injection time for a complete fill, we get an injection rate ~ 50 Amp/hour. This injection rate is quite demanding, particularly from the positron point of view, and, in order to reach this goal, we foresee for DAΦNE an injection system consisting of an e^+e^- LINAC followed by a DAMPING RING (DR). Such a solution will allow to obtain the desired positron accumulation rate by improving injection efficiency, repetition rate, positron flux and emittance etc, while keeping to a minimum the overall cost of the IS.

The complete injection scenario with the DR description can be found in Ref. [2], but let us recall the values of the main parameters that we will use in order to carry out the positron LINAC specifications:

Main ring & DR injection Energy	510 MeV
Mode of filling	One bunch at the time
LINAC macropulse length	t_L= 10 ns
Emittance/π	≤ 3.2 mm-mrad
Energy spread	ΔE/E ≈ ±1.0 %
DR(LINAC) injection repetition rate	f_L= 50 Hz
Main ring injection repetition rate	f_M= 1 Hz
Number of e^+/bunch into the main ring	N_b= 8.9 10^{10} => Q_b= 14 nC
Number of bunches into the main ring	h = 120
Main ring positron filling time	T = 360 sec

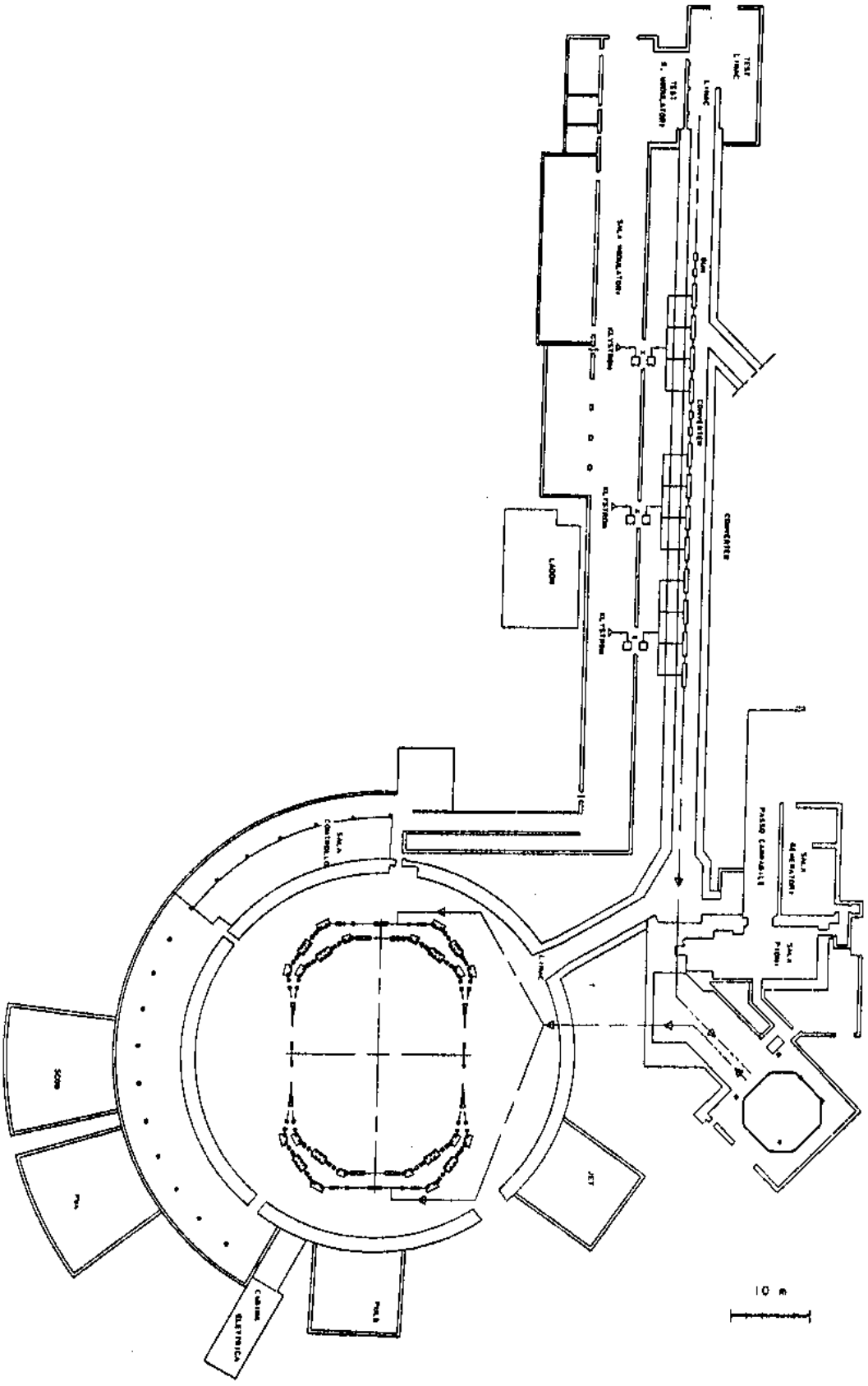

Fig. 1 - Schematic Layout of the DAΦNE Injection System

The schematic layout of the DAΦNE complex is shown in Fig. 1, while the main LINAC components are listed in the following :

- Thermionic gun
- Prebuncher at the main LINAC frequency f = 3 GHz.
- Standing Wave (SW) or Traveling Wave (TW) graded-β buncher at f=3 GHz.
- High current TW LINAC with output energy ≥ 250 MeV .
- Positron converter
- Capture section
- Low current e^+e^- TW LINAC with output energy ≥ 510 MeV.

2 - LINAC CHARGE REQUIREMENTS

Let us now, going back from the main ring to beginning of the LINAC, evaluate, along the IS, the electron and positron bunch charges needed to accumulate, into the main ring, the maximum number of positrons within the time T. In order to make this evaluation, we assume the following "standard" efficiencies

Transport and injection into main ring	$\eta_{MR} = 0.8$
Extraction from the DR	$\eta_{ex} = 0.9$
Injection into the DR	$\eta_{idr} \geq 0.5$
Converter to DR transport	$\eta_{ldr} = 0.9$
Positron conversion @ 250 MeV	$\eta_c = 8.0\ 10^{-3}$
Gun to converter electron transport	$\eta_{gc} = 0.4$

Let us first evaluate the positron charge in one LINAC macro-bunch:

$$Q^+ = \frac{h f_M Q_b}{\eta_{idr}\eta_{ldr}\eta_{ex}\eta_{MR} T f_L} = 0.3\ \text{nC} \quad \Rightarrow \quad 1.9\ 10^9\ e^+$$

Before to evaluate the electron charge Q^-, impinging the electron-positron converter, let us first point out that Q^- is related to the positron conversion efficiency η_c which is about proportional to the energy of incident electrons (for energies higher than few hundreds of MeV) and it depends on the collection, focusing and acceleration of produced positrons. The most frequently quoted number for η_c is:

$$\eta_c = 2 \cdot 10^{-2}\ E_c(\text{GeV}) \quad [e^+ \text{ in } \pm 1\% \text{ per electron}]$$

where E_c is the electron energy at the converter target. This value, obtained at ADONE and LEP injector [3], can be increased by a better positron focusing, using a flux concentrator, and by a strong acceleration through a short capture section with a very high field gradient of the order of 50 MV/m. This technique should allow, at least, an improvement factor of about 50% [4] in the conversion efficiency, which, taking E_c = 250 MeV, becomes:

$$\eta_c \approx 8 \cdot 10^{-3} \quad [e^+ \text{ in } \pm 1\% \text{ per electron}]$$

We shall use this value to calculate the gun emitted current. Nevertheless, we remind that the energy conversion should be the highest possible, compatibly with the cost of the LINAC.

The electron charge per LINAC macro-bunch at the converter is then:

$$Q^- = \frac{Q^+}{\eta_c} = 38 \text{ nC} \quad \Rightarrow \quad 2.3\ 10^{11}\ e^-$$

and, assuming a transmission efficiency from the gun to the converter η_{gc} = 0.4, the charge per pulse emitted by the gun has to be:

$$Q_g = \frac{Q^-}{\eta_{gc}} = 95 \text{ nC}$$

corresponding to a gun peak current:

$$I_g = \frac{Q_g}{t_L} = 9.5 \text{ A}$$

Besides the above requirements, a lower limit to the field gradient in the accelerating sections must be established, due to the length of the tunnel which already exists in the LNF area (≈ 75 m).

The LINAC filling factor (i.e. the ratio between the active accelerating length and the overall length) strongly depends on the adopted particle focusing. In our case, due to high field gradients expected in the accelerating sections (see later), the installation of quadrupoles and triplets in the drift spaces is then recommended for focusing the particles, since the solenoidal focusing around the sections can facilitate sparking and break down inside them.

The estimated filling factor for the DAΦNE-LINAC is then 0.7 like in the LIL injector where the same focusing system has been adopted. Being the needed space for gun and converter about 5 m, the effective length of the LINAC is reduced to 70 m and the available active length of the accelerating sections will be around 50 m. Therefore, the average field gradient of the accelerating sections must be greater than 15 MV/m since the necessary total energy gain of both high current and low current LINAC is ≥ 760 MeV.

3. THE LINAC ACCELERATING STRUCTURE

The DAΦNE-LINAC will be composed by two parts:

- A high current electron LINAC for positron production.
- A low current electron and positron LINAC for final acceleration.

The energy conversion should be as high as possible and preferably not lower than ≈ 250 MeV. The output energy of the second LINAC has to be, at least, equal to 510 MeV, which corresponds to the energy of the Φ-meson production. The electron current accelerated in the first LINAC, which is needed to have the required positron production at the converter, is about 5 A.

The electron current, in both linear accelerators, will be limited by the maximum energy dispersion, due to the beam loading, acceptable by the DR and which is assumed to be within ±1% [2]. The limits of the electron current will be given later on, when the parameters of the accelerating structure will be defined.

We foresee to use TW accelerating structures, since they provide high energy gain per unit length for a given RF power. High input power at the sections is then required to produce the accelerating fields. The installation of Pulse Compression (PC) systems is also foreseen to enhance the klystron output power [3, 5, 6, 7].

For long accelerating structures, where the filling time t_f is comparable to the klystron pulse length, the gain in energy multiplication, due to the PC system, may be quite small. In fact, for pulse length of 4.5 μs, the energy multiplication is about 1.5 in the 4.5 m long LIL structures with t_f =1.2 μs, and it is 1.4 in the 5 m long LNF-LINAC sections. The length of the DAΦNE-LINAC sections must be optimized to have both the needed field gradient and the minimum number of klystrons.

In conclusion, 2π/3 TW accelerating sections are proposed for the LINAC since its shunt-impedance is close to the optimum.

We will make now further considerations about the opportunity of using either the constance impedance (CI) or the constant gradient (CG) travelling wave $2\pi/3$ structure.

According to the analysis given in [7], the CI $2\pi/3$ structure, followed by a PC system, can give higher energy per input power and it has also a more uniform effective accelerating gradient along the structure compared with the gradient of the CG structure. Moreover, the construction of the CI sections is easier because the structure is more geometrically homogeneous, since it has no size variations along the beam axis direction. However, beam instabilities, namely beam break-up, can more easily take place in CI sections due to their geometrical homogeneity.

On the contrary, important advantages of the CG structures are their lower sensitivity to frequency deviations and the lower beam loading derivative.

New type of S band structures, $3\pi/4$ and $4\pi/5$ backward TW, are to date under development at GE/CGR-MEV with the collaboration of LAL (Orsay) [8]. Such structures seem to have a better shunt impedance and even better group velocity, but a lower possible maximum field gradient with respect to the $2\pi/3$ TW structures. In addition, these new structures have not yet been tested in normal operating condition, i.e. in presence of bunched beams, therefore no data are available on instabilities and beam break up. On the contrary, the $2\pi/3$ CG structure has been successfully tested in large linear accelerators like SLAC, LEP and DESY.

For all these reasons we propose to adopt constant gradient $2\pi/3$ TW accelerating structures in the DAΦNE-LINAC.

3.1. *Length and gradient optimization for the constant gradient* $2\pi/3$ TW *accelerating sections*

We have analyzed which CG accelerating section would have been better for DAΦNE linac. The details of this analysis are given in the next paragraph. Here we summarize the most important conclusions of our considerations. The following assumptions have been made:

accelerating sections:

length	L = 2 m, 2.5 m, 3 m, 4.5 m
quality factor	Q = 15000
beam pulse duration	t_L = 10 ns

klystron parameters:

output power	P = 45 MW, (PC input power = 40 MW)
pulse duration	T_k = 4.5 μs
storage cavity quality factor	$Q_c = 10^5$

Some important parameters of the sections are given below.

TABLE I

Section length (m)	Number of sect. per klystron	Without P.C.		With P.C.		Energy multipl. factor M
		E_{av} (MV/m)	Energy (MeV)	E_{av} (MV/m)	Energy (MeV)	
2	4	13.7	27.4	26.7	53.4	1.95
2.5	4	12.8	32.0	23.7	59.2	1.85
3.0	4	12.1	36.2	21.2	63.7	1.76
2.0	2	19.4	38.7	37.7	75.5	1.95
2.5	2	18.1	45.3	33.5	83.7	1.85
3.0	2	17.1	51.2	30.0	90.1	1.76
4.5	2	14.4	66.7	21.5	96.7	1.45

Taking the data of Table I, different possible configurations, presented in next chapter, can be proposed to fulfil the DAΦNE-LINAC requirements. We present here some of them, based on the 3 m long section which seems to be the most suitable for our purposes. We remark that Table II is based on the following conditions:

- The energy conversion is at least 270 MeV.

- The output positron current is greater than 30 mA.

The positron current is calculated with the formula

$$i^+ = 0.9\, i^-\, \eta_c\, E_c$$

where $\eta_c = 3.2 \cdot 10^{-2}/\mathrm{GeV}$ corresponds to a positron energy dispersion $\Delta E/E = \pm 1\%$.

The coefficient 0.9 takes into account the effective energy conversion due to the beam loading as it is calculated below.

TABLE II - Some possible configurations for the DAΦNE-LINAC based on the 3 m long accelerating sections.

N° sect.	16+2*	14+2*	12+2*	12+2*	10+2*
E (MV/m)	21	21	21	30	30
i+ (mA)	68	50	36	74	50
Wc (MeV)	520	390	270	560	380
Wt (MeV)	1060	930	810	1120	940
N° Klystrons**	4(4)+1(2)	4(4)	3(4)+1(2)	6(2)+1(2)	5(2)+1(2)
Cost(rel.)	1	.86	.82	1.085	.93

* 20 MeV Bunchers

** In brackets the number of sections per klystron

The LINAC configurations presented in Table II fulfil the above mentioned conditions. Additional informations, like reliability and costs, are then necessary to support the final choice. From this point of view, the solutions performing lower gradient, i.e. 21 MV/m, are preferable.

In fact:

- Most of the existing large electron LINACS usually operate at field gradient close to 10 MV/m.

- The existing tunnel in the LNF area allows the installation of about 50 m of active LINAC which means a possible total energy of 1000 MeV with an accelerating field of 20 MV/m.

- As shown in Table II, we estimate that the 20 MV/m linac is cheaper than the 30 MV/m solution.

The most attractive proposal, among those at 21 MV/m, is the one with the smallest number of sections (12+2), because it provides the needed positron current of 30 mA, with the least estimated cost. It should also be emphasized that whether a larger beam energy dispersion could be accepted by the DR (i.e. ±1.5%), proportionally larger positron current would be accepted. Thus, three new different possibilities are open:

- to proportionally decrease the main rings filling time below 360 sec.
- to decrease the necessary gun emitted current.
- to eventually reduce the energy conversion below 250 MeV with a reduction of the cost.

The schematic layouts of two possible solutions for a field gradient of 21MV/m are given in Figs. 2 and 3.

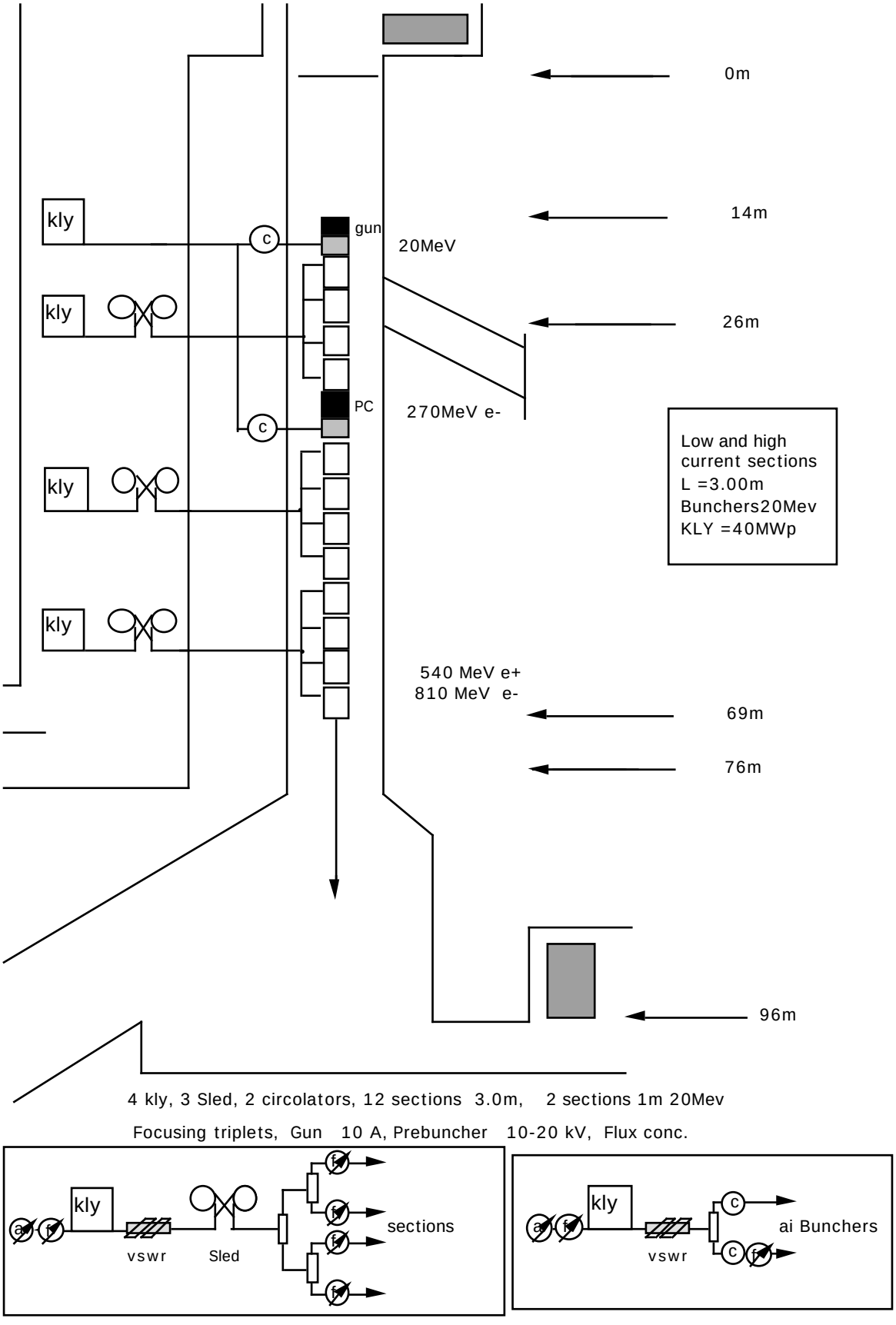

Fig. 2 - First DAΦNE-LINAC arrangement with 12 TW *3 m long sections + 2 bunchers.*

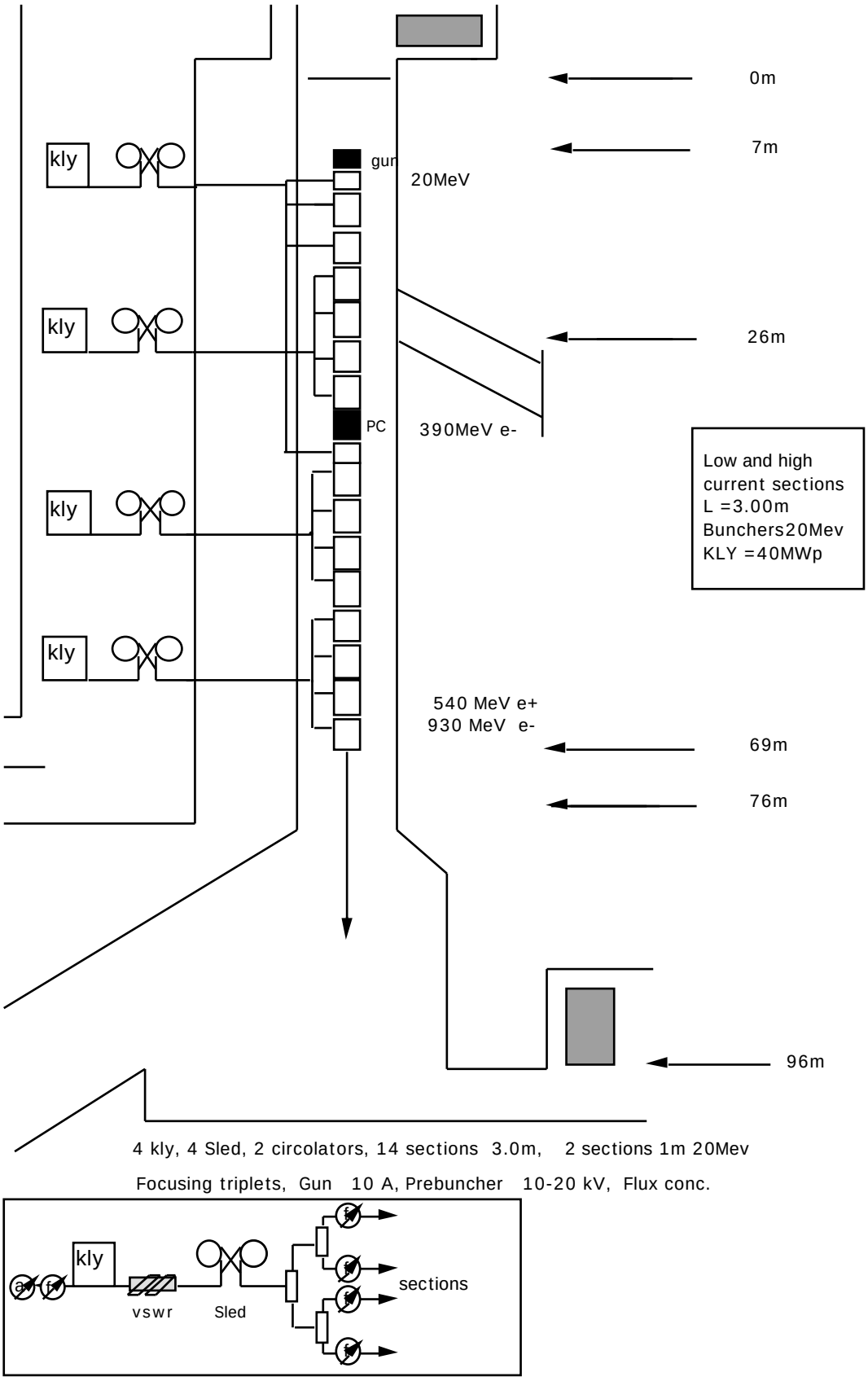

Fig. 3 - Second DAΦNE -LINAC configuration including 14 TW *3 m long sections and 2 bunchers.*

4. MAIN COMPONENTS OF THE INJECTION SYSTEM

4.1. *The Gun*

A single gun, dimensioned for the maximum peak current, needed during positron operation can be used.

The gun must transmit a current pulse $I_g \approx 10$ A for 10 ns up to 50 Hz of repetition frequency. These parameters are very close to the existing ADONE-LINAC gun. They could also be obtained, with larger cathode diameter, in a gun like the one described in Ref. [9]. The main gun parameters are listed in Table III.

TABLE III - Proposed gun parameters

Type	Pierce, triode
Spherical radius of the cathode	R_k = 40 mm
Cathode diameter (height)	D_k = (25÷30) mm
Anode potential	U_a = 100 kV
Current	I_g = 10 A
Emittance (invariant)	ε_n = $1 \cdot \pi \times 10^{-4}$ m.rad.
Macrobunch length	t_g = 10 ns
Repetition rate	f_r = 50 Hz

4.2. *The Bunching System*

The purpose of this system is to bunch the 'continuous' electron current emitted by the gun in a train of micropulses corresponding to less than 15 degrees of the period of the LINAC radiofrequency (about 14 ps) and to accelerate the particles to few MeV, before entering the constant phase velocity (v = c) accelerating structure of the LINAC.
It will consists of a prebuncher followed by a 20 MeV buncher.

4.2.1. The Prebuncher

The prebuncher is a TM_{010} mode single cell cavity resonating at the 2998.5 MHz LINAC frequency. The axial electric field created at the 1 cm cavity gap is in the range 10÷20 kV. The cavity is followed by a drift space D ≈ 25÷15 cm.

The prebuncher compresses 70% of the total bunch charge into about 20 degrees of the RF period, after passing across the drift space D. The following buncher section then further squeezes the bunch. Magnetic focusing is necessary to confine the beam in the transverse plane, in order to counteract the space charge forces in the low energy (100 keV) region from the gun. In order to avoid emittance deterioration, this magnetic field has to be properly matched to the magnetic field of the gun and the buncher.

4.2.2. The Buncher

The buncher rapidly accelerates low energy particles up to relativistic velocities (about 5÷20 MeV) in order to minimize the high current space charge effect and to provide additional axial phase contraction of the bunch. The buncher can be a short (~1 m) SW or TW accelerating section with a few graded-β cells. The SW solution is considered more convenient for short high gradient sections. The buncher input power may be more than 10 MW depending upon the required output energy.

The bunching process, considered before, is due to the variations of the electron velocity in relation to their energy. This process stops at relativistic energies when the electron velocity is practically constant and it is equal to the velocity of the light. The phase length of the bunch must therefore be lower than 15 degrees at the buncher output, corresponding to the required ±1% energy spread.

4.3. *Choice of the Accelerating Section Parameters,*

The main parameters of the DAΦNE-LINAC are similar to those of the injector LINAC for LEP [3], whose good performances we have considered as a reference. A careful optimization of the accelerating cells was done at LAL (Orsay) [10], in order to improve the RF parameters, i.e. the quality factor Q, the ratios r/Q and E_z/E_{max} (where r is the structure shunt impedance, E_z the axial accelerating field and E_{max} the peak field on the walls). The resonant frequency is f = 2998.5 MHz ($\lambda \approx 10$ cm). The electric field intensity E and the voltage gain V in a CG structure for low current operation can be calculated by means of the following expression:

$$E = \sqrt{\frac{P_o\ r}{L}\left(1 - e^{-2\tau}\right)} \approx \text{constant} \qquad (1)$$

$$V = \sqrt{P_o\ r\ L\ \left(1 - e^{-2\tau}\right)} \qquad (2)$$

The electric field, which is given in eq. (1), is considered almost constant due to the small dimensional variations of the iris and outer diameters 2a and 2b along the structure.

P_o is the input power at the section entrance, r is the average value of the effective shunt impedance, L is the section length and τ is the attenuation coefficient of the section given by

$$\tau = 0.5 \ln \left[1 + \frac{2 \pi L c}{Q \lambda v_{gL}} \right] \qquad (3)$$

where

- Q - quality factor of the accelerating section
- c - velocity of light
- λ - field wave-length
- v_{gL} - group velocity at the section output; it can be calculated from:

$$\frac{v_{gL}}{c} = \frac{2 \pi L}{Q \lambda} \frac{e^{-2\tau}}{1 - e^{-2\tau}} \qquad (4)$$

The group velocity at the section entrance is then

$$\frac{v_{go}}{c} = \frac{v_{gL}}{c} e^{-2\tau} = \frac{2 \pi L}{Q \lambda (1 - e^{-2\tau})} \qquad (5)$$

In CG structures and for a given length L, the above parameters are related to the iris diameter 2a. The diameter 2b of the waveguide should also variate with 2a to keep the resonant frequency constant along the section . Usually, there is only one limitation concerning the iris diameter 2a, namely it should be sufficiently large to allow the electron beam to pass freely through the section.

We assume a minimum value 2a =18 mm (identical diameter is used in LIL injector linac). The following approximate laws, relating the diameter 2a to other parameters, have been carried out at LAL[10] using the SUPERFISH code, for $18 \leq 2a \leq 26$ mm:

$$2b = 80.065 + 0.135(2a) - 0.00366(2a)^2 + 0.0001827(2a)^3 \qquad (6)$$

where 2a and 2b are in mm

$$r\ [M\Omega/m] = 86 - 3.6\ (2a)^2 \qquad (2a \text{ in cm}) \qquad (7)$$

$$\frac{v_g}{c} = \frac{(2a)^{2.3}}{891} \qquad (2a \text{ in cm}) \qquad (8)$$

$$Q = 15200.$$

The parameters of the $2\pi/3$ TW structure have been calculated with the OSCAR-2D code [11, 12], for different iris diameters, in order to confirm the validity of the previous expressions. The results obtained with (6) and (7) are compared in Table IV with those given by the code. The variation of the resonant frequency is less than 0.5 MHz for different iris diameters and corresponding variations of the outer diameter 2b. Moreover, the shunt impedance values calculated with the formula (7), differ less than 1 MΩ/m from the code computations.

TABLE IV- Variations of 2b as a function of 2a to keep the frequency of the mode $2\pi/3$ constant .

2a mm	18	20	22	26
2b mm(eq.6)	82.30	82.7886	83.2155	84.32
f [MHz]	2999.78	3000.20	3000.21	2999.72
r_{sh} [MΩ/m] eq. (7)	74.34	71.6	68.58	61.66
r_{sh} [MΩ/m] (OSCAR)	75.48	72.6	68.03	62.4
Q (OSCAR)	15180	15214	15238	15315

The validity of the formula (8) to evaluate the group velocity has also been checked by calculating the dispersion curve for two values of 2a (20 mm and 26 mm) with OSCAR-2D [11]. For comparison, an analytic expression of the dispersion curve has also been used [12]

$$\omega_\phi^2 = \omega_o^2 + 0.5\,(\omega_\pi^2 - \omega_o^2)\,(1 - \cos\phi) \qquad (9)$$

The shape of the dispersion curve is defined by two frequencies f_o and f_π corresponding to the modes 0 and π.

TABLE V- Dispersion curve [$\omega = F(\phi)$] mode comparison as calculated by the program OSCAR-2D and by Eq. (9).

Mode ϕ	2a = 20 mm Frequency f calculated by OSCAR MHz	2a = 20 mm Frequency f calculated by Eq. (9) MHz	2a = 26 mm Frequency f calculated by OSCAR MHz	2a = 26 mm Frequency f calculated by Eq. (9) MHz
0	2975.54	2975.54	2938.23	2938.23
$\pi/3$	2983.80	2983.80	2958.81	2983.78
$2\pi/3$	3000.20	3000.25	2999.25	2999.45
π	3008.44	3008.44	3019.58	3019.58

Table V gives the comparison of the modes of the dispersion curve $\omega = F(\phi)$, calculated with the program OSCAR-2D and by the equation (9) for two values of 2a: 20 mm and 26 mm.

In both cases, the agreement between the dispersion curves is excellent at the intermediate points $\phi = \pi/3$ and $\phi = 2\pi/3$.

Due to the smoothness of both curves, also their first derivatives $d\omega/d\phi$ should be almost equal. We may then use the analytical expression (9) to compute $d\omega/d\phi$, necessary to define the group velocity.

Denoting by $\beta = \phi/h$ the propagation constant of the structure, where h is the distance between the irises, and using the Eq. (9), we get:

$$\left(\frac{v_g}{c}\right)_\phi = \frac{1}{c}\frac{d\omega_\phi}{d\beta} = \frac{h}{c}\frac{d\omega_\phi}{d\phi} = \frac{2\pi h}{c}\frac{f_\phi^2 - f_o^2}{4 f_\phi \sin\phi} \qquad (10)$$

Substituting the values of the ϕ mode frequencies f_ϕ of Table V in the expressions (8) and (10) and taking h = 0.033326 m, we have the group velocities shown in Table VI.

TABLE VI - Dependence of the group velocity v_g on the iris diameter.

2a (cm)	2.0	2.6
$v_g/c = (2\pi h/c)\, df/d\phi$	0.992×10^{-2}	2.262×10^{-2}
$vg/c = (2a)^{3.23}/891$	1.05×10^{-2}	2.46×10^{-2}

The results in Table VI are in appreciable agreement even though the approximate formula (8) gives a group velocity higher 6.8% than that given by Eq. (10).

In conclusion, rapid estimation of the CG structure main parameters may be done, with possible small corrections of the group velocity, by using the approximate formulae (6-8) given for the LIL accelerating sections. The results of these calculations are presented in the Table VII.

TABLE VII - Main parameters of the CG accelerating sections under consideration for the DAΦNE-LINAC.

L [m]	2	2.5	3	4.5
2τ	.75	.8747	.985	1.2575
$g = 1 - e^{-2\tau}$	.5276	.583	.6266	.7156
$T_f = 2\tau Q/\omega$ [μs]	.5970	.697	.784	1.00 (1.2)*
$2a_{max}$ [cm]	2.27	2.36	2.44	2.66 (2.5)**
r_{shunt} [MΩ/ml	71.0	70.3	69.7	69.2
P_o = 10 MW				
E [MV/m]	13.69	12.81	12.06	10.49
V [MV]	27.37	32.0	36.2	47.2
P_o = 20 MW				
E [MV/m]	19.35	18.11	17.06	14.84
V [MV]	38.71	45.25	51.2	66.76

* T_f =1 μs in the case of a continuous change in the structure iris diameter; T_f =1.2 μs for finite steps in iris diameter; the LIL structure has 9 parts with different iris diameter between 2.5 cm and 1.8 cm.

** 2a = 2.66 cm is given by eq. (8); 2a = 2.5 cm is the value we propose.

Other parameters kept constant during the calculations are:

- Frequency f = 2998.5 MHz corresponding to the wavelength λ = 10 cm.
- Minimum iris diameter $2a_{min}$ = 1.8 cm.
- Quality factor of the structure Q = 15000.
- Klystron output power 40 MW feeding either 4 sections (10 MW per section) or 2 sections (20 MW per section without PC).

Table VII shows that even at 20 MW per section, the highest field intensity in the shortest 2 m section is lower than 20 MV/m without PC. This implies that the installation of the PC system, in order to reduce the klystron number, is essential.

4.3.1. Pulse Compression System for the DAΦNE-LINAC

According to the theory developed by Farkas et al. [5], the energy multiplication factor M in the case of a CG-TW accelerating section is given by

$$M = \frac{V_{max}}{V_o} = \gamma \frac{(1-g)(1+\nu)}{g(1+\nu)} e^{-(T_f/T_c)} - (\alpha-1) \qquad (11)$$

where:

V_{max} = maximum voltage gain with PC
V_o = maximum voltage gain without PC
α = $2\beta/(1+\beta)$
β = storage cavity coupling coefficient
T_c = $2Q_L/\omega = 2Q_c/\omega\,(1+\beta)$ storage cavity filling time
Q_c = unloaded cavity quality factor
Q_L = $Q_c/(1+\beta)$ loaded cavity quality factor
ω = $2\pi f$, with f = resonant frequency
γ = $\alpha\,[\,2-\exp(-\tau_1)\,]$
τ_1 = t_1/T_c, with t_1 = starting time of the cavity discharge
T_f = $2\tau Q/\omega$ accelerating section filling time
τ = attenuation constant of the accelerating section
g = $1-\exp(-2\tau)$
Q = quality factor of accelerating scction
ν = $T_f / [\,T_c \ln(1-g)\,] = -Q/\nu\, T_c = -Q\,(1+\beta)/2Q_c$

As shown in Eq. (11), the energy gain M is a rather complicated function of several factors depending on the parameters of the storage cavities, the accelerating section and the klystron pulse length.

To analyze the behaviour of the PC system, two code programs have been developed elsewhere [12, 13]. They allow to follow the evolution time of the system and find the optimum set of parameters that make possible the maximum energy gain or the minimum energy dispersion due to the beam loading.

Calculations of the optimum cavity coupling β and the corresponding energy multiplication factor M are presented in Table VIII, for three sections of different length L and two klystron pulse lengths T_k.

TABLE VIII - Energy multiplication coefficient M corresponding to the optimum coupling β as a function of the storage cavity quality factor Q for different section lengths and klystron pulse durations.

Tk = 4 μs						
L (m)	2.5		3		4.5	
$Q/10^5$	β_{opt}	M	β_{opt}	M	β_{opt}	M
1.O	5.0	1.80	4.5	1.71	3.5	1.39
1.l	5.5	1.82	5.0	1.72	3.5	1.40
1.2	6.0	1.83	5.5	1.73	4.0	1.41
1.3	6.5	1.84	6.0	1.74	4.5	1.415
1.4	7.0	1.85	6.5	1.75	4.5	1.42
1.5	7.5	1.86	7.0	1.76	5.0	1.43
Tk = 4 .5 μs						
L (m)	2.5		3		4.5	
$Q/10^5$	β_{opt}	M	β_{opt}	M	β_{opt}	M
1.O	5.0	1.85	4.5	1.76	3.0	1.45
1.1	5.5	1.87	5.0	1.78	3.5	1.47
1.2	6.0	1.88	5.5	1.79	4.0	1.48
1.3	6.5	1.89	6.0	1.80	4.0	1.49
1.4	6.5	1.90	6.0	1.81	4.5	1.50
1.5	7.0	1.91	6.5	1.82	5.0	1.51

From Table VIII one deduces:

- There is an optimum value of the coupling b for which the energy gain factor M is maximum. The value of bopt increases with the storage cavity quality factor Qc, and decreases for longer pulse length and longer section length L.

- The energy gain factor M increases only about 3÷4 % for an increasing in Qc of 50 % (105 to 1.5 105).

- Shorter is the section (i.e. shorter filling time), higher is the energy gain per constant pulse duration.

- Moreover, the energy gain factor M grows with the pulse duration. The increasing of Tk from 4 to 4.5 ms has about the same effect on the factor M that one would has with an increasing of Qc from105 to 1.5105. There-fore, to obtain larger energy gain it is more convenient to use longer klystron pulses than higher quality factors of the storage cavities. This is the reason why (see below for further calculations) we will assume Qc =105.

Some important parameters of the four accelerating sections suitable for the DAFNE-LINAC have been calculated, using the data of Tables VII and VIII. The results of these calculations have been previously shown in Table I.

Taking the data in the Table I, different configurations are proposed for the DAFNE-LINAC. Some of them are presented in Table IX.

TABLE IX - Possible arrangements for DAFNE-LINAC.

Section Length	No. of Sections per Klystron	No. of High Current Sections	Convers. Energy Wc MeV	No. of High Energy Sections	Output Energy MeV	Total Number of Klystrons	Total Number of Sections	Linac Length m
2.5	4	6	375	10	612	5	16+2	40+2
2.5	4	7	434	9	553	5	16+2	40+2
3.0	4	8	530	8	530	5	16+2	48+2
3.0	4	6	400	8	530	4	14+2	42+2
3.0	4	4	270	8	530	4	12+2	36+2
3.0	2	6	560	6	560	7	12+2	36+2
3.0	2	4	380	6	560	6	10+2	30+2
4.5	2	4	410	6	600	6	10+2	45+2
4.5	2	6	600	6	600	7	12+2	54+2

The choice of the LINAC structure among the proposed arrangements depends upon which parameter we want to take for reference.

If the LINAC length must be short, the solution presented in the 2nd row of Table IX guarantees adequate conversion and output energy. The average field gradient (≈ 24 MV/m) is however a little high.

For an active length of about 50 m (the focusing adopted is important in this case), the best arrangement uses the 3 m sections. We present 3 low field layouts (1 Klystron per 4 sections) and 2 high field configurations (1 klystron per 2 sections).

The DAΦNE injection requirements are fulfilled in any case, and the choice should be made on the base of reliability and cost. From this point of view, the low gradient case with 14 or 12 TW sections is the best solution (see Table II).

The use of 4.5 m structures is also considered in Table IX (it is the solution adopted for LEP), but the installation of the PC system is less effective in this case. The configuration using (4+6) sections, is comparable with the (6+8) 3 m sections. The cost of two additional klystrons is partially compensated by the lower number of sections, 10 instead of 14.

4.4. *Beam Loading and Energy Dispersion.*

The transient Beam Loading (BL) has not been taken into account up to now and the above considerations were made for low current regime.

However, during the operation of the DAΦNE-LINAC, the BL cannot be neglected, especially in the positron mode, when heavy BL occurs in the electron linac before the positron converter, where intense bunch charges, of the order of 100 nC, must be accelerated.

In the electron operation mode the transient BL will limit the maximum electron current which can be accelerated within ± 1% of energy dispersion.

Since the SW structures may be used like bunchers, we will consider the BL both in SW and TW accelerating sections.

4.4.1. Beam Loading in SW Accelerating Sections

SW accelerating sections can be used to bunch the particles in the high current part of the electron linac and to capture them after the positron converter. The BL in such accelerating structures is treated in [14] and we shall use here the results obtained there.

Let us denote by E_o the electric field intensity in the SW section before the bunch enters it and by E_1 the field after the last electron has left. Assuming that the average field acting on the bunch is

$$E_q = \frac{E_o + E_1}{2}$$

we obtain the following equation for E_1:

$$E_1^2 - E_o^2 + r\,\omega\,TTF\frac{q\,(E_1 + E_o)}{2\,Q} = 0 \qquad (12)$$

where

$$E_o = \sqrt{\frac{P\,r}{L}}$$

r - shunt impedance in [MΩ/m]
P - section input power in [MW]
q - bunch charge [C]
ω - angular frequency
Q - cavity quality factor
TTF - transit time factor which can be approximately calculated from

$$TTF = \frac{\sin(\pi\, g/\lambda)}{(\pi\, g/\lambda)}$$

with

g - accelerating gap
λ - field wave-length.

The first electron then gains the energy:

$$eV_o = e\,TTF\,E_o\,L$$

and the last:

$$eV_1 = eTTF\,E_1\,L$$

The corresponding energy dispersion is then :

$$\frac{\Delta V}{V_{av}} = 2\,\frac{V_o - V_1}{V_o + V_1} = 2\,\frac{E_o - E_1}{E_o + E_1}$$

Taking r = 70 MΩ/m, Q = 15000, f = 2998.5 MHz, q = 100 nC, L = 0.7 m, g = λ/3 (TTF = 0.827) we can calculate the effect of the BL for different values of the power P.

The results are given in Table X.

TABLE X

P MW	E_o MV/m	E_1 MV/m	V_o MV	V_l MV	$\Delta V/V_{av}$ %
5	22.36	18.73	12.94	10.84	17.7
7.5	27.39	23.75	15.86	13.75	14.0
10.0	31.62	27.99	18.30	16.20	12.0
15.0	38.73	35.09	22.42	20.31	9.82

Section length of 0.7 m and 15 MW input power allow the energy to increase of about 20 MeV with energy spread lower than 10% even for bunch charge of 100 nC. In fact, the bunch charge will be rather lower since about 30÷40% of the electrons are usually lost in the first cells of the buncher.

4.4.2. Beam Loading in CG TW Sections

The voltage induced in a CG section by a bunch with current I_o, see reference [15], is given by:

$$V_b(t) = \frac{r\, I_o\, L}{2\, g} \left\{1 - \left[e^{-2\tau\,[(t-ti)/tf]} - 2\tau(t-t_i)\; e^{-2\tau\,[(t-ti)/tf]}\right]\right\} \qquad (14)$$

where:

t_b is the bunch length
t_f is the structure filling time
t_i is the bunch injection time
t is the attenuation coefficient defined in eq. (3)
$g = 1 - e^{-2\tau}$

By taking $t_i = t_f - t_b$ (i.e. we assume to inject the bunch one bunch length before the end of the filling time) the eq. (14) writes:

$$V_b(t_f) = \frac{r\, I_o\, L}{2g} \left[1 - e^{-2\tau x_b} - 2\tau x_b\, e^{-2\tau}\right] \qquad (15)$$

with: $x_b = t_b/t_f$.

The value of V_b for the three sections considered in Table IX, are presented in Table XI.

TABLE XI

L m	P MW	V_o MV	M	V_m MV	V_b/I_o MV/A	V_b/V_{oa} %	V_b/V_{ma} %
2.5	10	32.0	1.85	59.2	1.082	3.44	1.84
3.0	10	36.2	1.76	63.7	1.279	3.60	2.02
4.5	20	66.8	1.45	96.7	1.563	2.36	1.63

V_{oa} and V_{ma} are defined as follows:

$$V_{oa} = V_o - 0.5V_b, \quad V_{ma} = V_m - 0.5V_b$$

The ratio V_b/I_o is the BL for 1A beam current and a pulse duration t_b=10 ns.

The energy dispersion $\Delta V/V_{av}$, due to the BL, is inversely proportional to the field intensity in the section, as shown in Table X. Then, since the BL depends on the beam current and cavity length and it does not depend on the field gradient, this can be increased by means of PC devices in order to get a lower energy spread.

The heaviest BL occurs, in the positron operation mode, in the LINAC section located before the converter where the beam current is estimated around 5 A and induces a transient BL of 12% in the 4.5 m long structure and 18% in the 3 m one, when used without PC. On the contrary, these values will respectively decrease to 8% and 10% with PC.

We can now estimate the maximum admissible electron current (during the electron mode of operation) to have an energy dispersion lower than ±1%.

Let us consider the 3 m section layout. The use of the PC scheme allows the energy dispersion to be within ±2% for a current of 1 A. *If the energy spread was due only to the beam loading then*, taking an electron current of 0.5 A, we would fulfil *the* required *condition* of ±1% of energy dispersion. Since there is also energy spread due to the phase *dispersion*, *then taking for instance* the worst case that, both effects are equal and add together, the maximum electron current should be lower than *0.25 A* to have ±1% of energy dispersion. This current value is still more than 5 times larger than the maximum positron current so that the electron filling time can be further reduced.

4.5. *Positron Source*

The main components of the positron production system are:

- the converter
- the magnetic focusing
- the high gradient capture accelerating section

4.5.1. Converter and magnetic focusing

The average power of an electron beam of energy E_c, passing through the converter, is:

$$Pc = E_c\, I_g\ \eta_{gc}\ t_L\ f_L = 1.2\ kW$$

if we take, for safety, the values:

$$E_c = 500\ MeV,\quad I_g = 12A,\quad \eta_{gc} = 0.4.\ ,\ t_L = 10ns\ \text{ and }\ f_L = 50\ Hz.$$

The power dissipated in the converter is a fraction of that of the striking beam. The energy lost by high energy electrons is mainly due to Bremsstrahlung . In heavy elements like W, Au or Pb, this is true at energies higher than about $20 \cdot m_o c^2$ [16]. The average energy loss per cm is given by

$$-\frac{dE}{dx} = N\, E\, \Phi_{rad}$$

where N is the number of atoms per cm^3, E is the energy of the impinging electrons and Φ_{rad} is the Bremsstrahlung cross section.

Φ_{rad} is practically independent [16] on the energy of the electrons for sufficiently high energies, i.e. for $E >> Eo = 137 \cdot m_o c^2 \cdot Z^{-1/3}$ being Z the atomic number of the target material, corresponding to $Eo \approx 32 m_o c^2$ for gold.

In agreement with this and according to [16] for Ec >100 MeV, the fraction of power deposited in the converter is constant and equal to ~16%, provided that the thickness of the converter is properly chosen, i.e. proportionally to the primary energy of the beam.

In our case the power to dissipate on the target is:

$$Pd \approx 0.16 \times 1.2\ kW = 192\ W$$

This is much less than the power dissipation design of the ADONE converter (about 3 kW). Considering the good thermal properties of the ADONE converter, we propose to adopt a similar solution for DAΦNE.

A sketch of the target is shown in Fig. 4 and includes two possible solutions for the positron focusing: flux concentrator and pulsed magnetic lens. Considering the higher energy conversion respect to ADONE (~ 250 MeV instead of 100), the thickness of the converter target should be larger, e.g. ~ 2 radiation length instead of about one.

For a good positron production efficiency, the diameter of the electron spot on the converter should be of the order of 1 mm , obtainable with a special focusing system consisting of quadrupole triplet. However, one must also take into account that the spot diameter has to be not less than 1 mm, otherwise the power density could cause excessive thermal stress and eventually damage the target itself.

To optimize the positron capture efficiency , the converter should be closely followed by a very intense tapered solenoidal magnetic field of the order of 5÷6 Tesla. This can be generated by a so called flux concentrator similar to that employed at SLAC.

A scheme of the configuration including converter, flux concentrator and capture section is shown in Fig. 4. The magnetic field of the flux concentrator must be matched to the solenoidal field of the capture section according to the following Table XII.

TABLE XII

Flux concentrator field	5.8 T
Tapered solenoid field	1.2 T
Uniform solenoid field	0.5 T

An additional optimization of the capture efficiency can be obtained by adding to the flux concentrator a very short high-field accelerating capture section. The main requirements of this section must be:

- High field gradient: $E > 30$ MV/m
- Short length: $L \approx 1.5$ m.

Different types of accelerating structures can be chosen to fulfil the above requirements, e.g. travelling wave (TW) constant gradient (CG) or constant impedance (CI) structures or standing wave (SW) structures [18].

A preliminary discussion on the choice of the accelerating structure is given in [19]. According to the results obtained there, for a length L=1.5 m and input power P=30 MW, we get:

E = 22 MV/m, W = 32.6 MeV for CG TW section and
E = 30 MV/m, W = 46 MeV for SW $\pi/2$ biperiodic SW section.

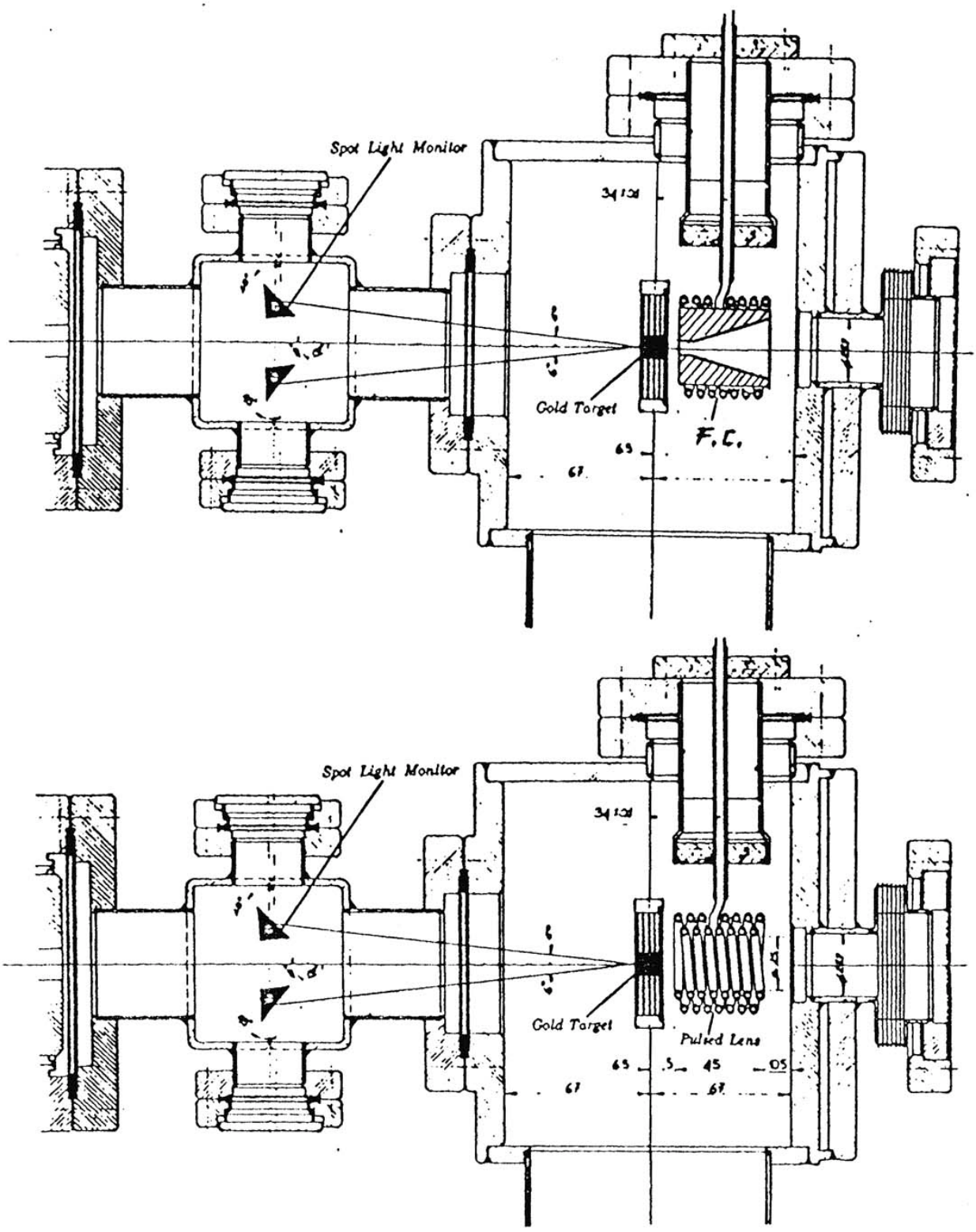

Fig. 4 - Sketch of the ADONE e^- e^+ Converter.

REFERENCES

[1] S. Bartalucci et al.: "DAΦNE Design Criteria", DAΦNE Technical Note G-2, Nov. 1990.

[2] M. Preger: "A Positron and Electron Ring for DAΦNE", DAΦNE Technical Note I-l, Nov. 1990.

[3] J.H.B. Madsen: "LEP Injector Linacs", CERN PS 89-56 (LP).

[4] J.E. Clendenin: " High-Yield Positron Systems for Linear Collider" SLAC-PUB-4743, April 1989.

[5] Z.D. Farkas et al.: "SLED: A Method of Doubling SLAC'S Energy", Proc. 9th. Int. Conf. on H.E.A., Stanford Calif., May 2-7, 1974.
Z.D. Farkas et al.: Recent Progres on SLED the SLAC Energy Doubler. IEEE Trans. on Nuclear Science, NS-22, N. 3 June, 1975.

[6] A. Febel: "Linacs Upgraded", DESY Journal 85/2 p. 6.

[7] J. Le Duff: "Optimization of TW accelerating Sections for SLED type operation", Linear Accelerator Conference, Darmstadt 1984.

[8] G. Bienvenu, P. Brunet: "Operational Limits of High Accelerators Gradients", Proc. EPAC 90, Nice 1990.

[9] S. Kulinski, M. Vescovi: "A Gun For LISA", LNF-87/98(R), 16 Nov.1987.

[10] R.Belbeoch et al.: "Rapport d'Etudes sur les Projet des Linacs Injecteur de LEP (LIL)", LAL/RT82-01, Janvier 1982.

[11] P. Fernandes, R. Parodi: "LALAGE - A Computer Program to Calculate the TM Modes of Cylindrically Symmetrical Multicell Resonant Structures", PAC 1982, Vol. 12, pp.131-137.

[12] S. Kulinski et al.: "Linac for Afrodite, Solution with Pulse Compression" Memo AF-13, Frascati 30 October, 1986.

[13] B. Spataro: "Studio di un Sistema per Aumentare I'Energia del Linac di Frascati", Nota Int. LNF-84/12(R).

[14] P. Brunet: "Section Accelerateur Fort Courant en Ondes Stationnaires" LAL/PI/80-20, Orsay May 1980.

[15] J.W. Wang: "R.F. Properties of Periodic Accelerating Structures for Linear Colliders", SLAC Rep. 339, July 1989.

[16] W. Heitler: "The Quantum Theory of Radiation", Oxford 1966.

[17] F. Amman: "Positron Accelerators in Linear Accelerators", edited by P. Lapostolle and A.L. Septie, North Holland 1970.

[18] H. Hoag: "Notes on the RF System for the SLC Positron Source. Single Pass Collider", Memo CN-282, SLAC 17 Oct. 1984.

[19] S. Kulinski: "Some Remarks on Positron Creation and Acceleration in the Injection System of ARES Φ-Factory", Memo ARES-19, Frascati Nov. 1989.

DAΦNE LINAC Performance Specifications

1) *Equipment*	
Frequency	2.9985 GHz
Frequency stability of pilot oscillator (1 hour)	$\leq 10^{-8}$
Temperature stability of cooling water to accelerator guides, rectangular waveguides and coaxial drive cable.	± 0.1 °C
Pulse repetition rate at 4.5μs r.f. pulse	50 pps
Klystron pulse voltage stability bin for 4.5μs total pulse length at 45 MW peak r.f. power to accelerator at 50pps	± 0.25 %
Linac vacuum at full power	$5 * 10^{-8}$ Torr
Vacuum at the end of accelerator guide	10^{-7} Torr
(Axial magnetic field in positron lens)	(≥ 1.8 T)
Axial magnetic field in flux concentrator	≥ 5.5 T
Average axial magnetic field of long solenoid over sections (buncher) before and after converter	.25÷.5 T
Focusing system (before the positron converter)	Q-pole triplet
Focusing system (after the positron converter)	Q-poles
2) *High current sections*	
Total energy at zero current	≥ 270 MeV
Pulse current width	10 ns
Total energy at 150 mA	270 MeV
Total energy at 5 A	≥ 250 MeV
Diameter of focused beam on converter, 80% of 5A total current within	1 mm
Electron bunch width at converter, 80% of 5A total current	±8 degrees
Number of sections	4+1
3) *Low current sections*	
Total energy at zero current	540 MeV
Total energy at 150 mA	≥510 MeV
Number of sections	8+1
4) *Complete machine*	
Total length (from Gun to Linac output)	< 65 m
<u>Electron beam:</u>	
Electron energy at zero current	> 810 MeV
Electron energy at 150mA total electron pulse current	≥ 810 MeV
Electron pulse current at 510 MeV within ±0.5% energy	≥ 150 mA
Emittance (80% output current)	$< \pi * 10^{-6}$ m rad
<u>Positron beam:</u>	
Positron energy at zero current	> 510 MeV
Positron pulse current at 510 MeV within ±1% energy	≥ 36 mA
Emittance (80% output current)	$< \pi * 10^{-5}$ m rad